GA–A27320

MODELS OF SOL TRANSPORT AND THEIR RELATION TO SCALING OF THE DIVERTOR HEAT FLUX WIDTH IN DIII-D

by

M.A. MAKOWSKI[1], C.J. LASNIER[1], A.W. LEONARD[2], D. ELDER[3], T.H. OSBORNE[2], and P.C. STANGEBY[3]

JULY 2012

GENERAL ATOMICS

DISCLAIMER

GA–A27320

MODELS OF SOL TRANSPORT AND THEIR RELATION TO SCALING OF THE DIVERTOR HEAT FLUX WIDTH IN DIII-D

by

M.A. MAKOWSKI[1], C.J. LASNIER[1], A.W. LEONARD[2], D. ELDER[3], T.H. OSBORNE[2], and P.C. STANGEBY[3]

This is a preprint of a paper to be presented at the Twentieth International Conference on Plasma-Surface Interactions in Controlled Fusion Devices, May 21–25, 2012 in Aachen, Germany and to be published in the *J. Nucl. Mater.*

[1]Lawrence Livermore National Laboratory, Livermore, California, USA
[2]General Atomics, P.O. Box 85608, San Diego, California
[3]University of Toronto Institute of Aerospace Studies, Toronto, Canada

Work supported in part by
the U.S. Department of Energy
under DE-AC52-07NA27344 AND DE-FC02-04ER54698

GENERAL ATOMICS PROJECT 30200
JULY 2012

GENERAL ATOMICS

MODELS OF SOL TRANSPORT AND THEIR RELATION TO SCALING OF THE DIVERTOR HEAT FLUX WIDTH IN DIII-D

M.A. Makowski[a*], C.J. Lasnier[a], A.W. Leonard[b], D. Elder[3], T.H. Osborne[b], and P.C. Stangeby[c]

[a]*Lawrence Livermore National Laboratory, Livermore, CA 94550, USA*
[b]*General Atomics, PO Box 85608, San Diego, CA 92186-5608, USA*
[c]*University of Toronto Institute of Aerospace Studies, Toronto, Canada*

Abstract. A cross machine analysis of heat flux profile measurements has produced a particularly simple scaling law for the scrape-off-layer (SOL) width, going as $B_{p,mp}^{e}$ with $e \sim -1.0$ where $B_{p,mp}$ is the poloidal magnetic field at the midplane. This result is in very good agreement with a model based on drift-induced transport. We are also developing a model that extends the kinetic ballooning mode pedestal paradigm to the separatrix and into the SOL. We have calculated the critical pressure gradient at the separatrix using the BALOO code and found that it scales proportionately with the measured pressure gradient. Using an improved high rep-rate and higher edge resolution Thomson scattering system on DIII-D, it is now possible to make detailed comparisons of scrape-off-layer (SOL) profile characteristics with the heat flux profile. We find that a two-point flux-limited model is in better agreement with measurements than a conduction-limited model.

1. Introduction

Parallel heat flux to material surfaces is a critical design parameter for next step devices such as ITER, FNSF, and DEMO. There are few predictive scaling relations for the parallel heat flux and these vary in their dependencies. Heat flux profiles on DIII-D obtained from IR thermography [1] under controlled conditions reveal that the heat flux width scales as B_p^{-1}, essentially independent of all other physics and engineering parameters while the combined data of C-MOD, DIII-D, and NSTX [2] yields a stronger dependence of $B_p^{-1.5}$.

This result significantly reduces possible theoretical models explaining the physics setting the heat flux width. Two are of particular relevance. The first model posits that magnetic drifts carry particles into the scrape-off-layer (SOL) where they then flow into the divertor [3]. This model is in very good agreement with measurements [2]. The second model extends the kinetic ballooning mode (KBM) pedestal paradigm up to the separatrix and into the SOL. Evidence for this is that the critical pressure gradient computed from infinite-n ballooning mode theory scales proportionately with the measured separatrix pressure gradient.

Accurately defining the separatrix location is thus an important issue as the values of temperature and density and their scale lengths evaluated at the separatrix are needed to make meaningful comparisons with theory. However, these quantities are very sensitive to position due to the rapidly varying profiles at the pedestal to SOL transition. Pedestal and SOL profiles of unprecedented detail are now obtained routinely on DIII-D with an upgraded Thomson scattering system. The system features both improved edge spatial resolution through an increase in the number of

channels and increased time resolution by increasing the number of lasers. The effective spatial resolution is further increased by modulating the plasma boundary at the point it intersects the Thomson chord.

The new system has been employed to make detailed measurements of electron density and temperature profiles as plasma current and central density were varied. The fidelity of the measurements has enabled us to make careful comparisons with theory. Two-point models of parallel heat transport based on power balance provide a means of locating the separatrix. This type of analysis has been carried out for a pair of two-point models: a conduction-limited (Spitzer) model and a flux-limited model [4]. Here we find that the separatrix values of electron temperature and density have similar dependencies on the central density and plasma current, but the values of the separatrix density and temperature differ by up to a factor of 2.

The relationship between the measured heat flux width and that derived from the two-point models has also been explored. Comparison of the heat flux width with the conduction-limited and flux-limited widths reveals that the flux-limited estimate of the heat flux width is in better agreement than the conduction-limited estimate over the full range of our measurements.

2. Heat Flux Width Measurements and Models

Heat flux profiles on DIII-D are obtained using IR thermography [1]. The profiles are then fit to a two-parameter fitting function [5] in which one parameter characterizes the profile width in the private flux region, w_{pvt}, and the second in the SOL, λ_{sol}. An integral width (integral of the profile divided by the peak) can also be obtained and is given approximately by $\lambda_{\text{int}} \cong \lambda_{sol} + 1.64 w_{pvt}$ [2]. Regression of λ_{int} against engineering and physics parameters yields a strong dependence on I_p with weaker dependencies on several other parameters (such as B_t or P_{sol}). However, a particularly simple regression is obtained by considering λ_{sol} rather than the integral width. In this case, the poloidal magnetic field at the mid-plane, B_p, alone is found to be as good or better an ordering parameter for λ_{sol} than multiple-parameter fits of λ_{int} involving I_p. This is shown in Fig. 1 which plots λ_{sol} versus B_p together with a power law scaling $\lambda_{sol,fit} = C B_p^e$ with $e \sim -1$. A power law scaling against I_p alone yields $\lambda_{sol} = (2.67 \pm 0.10) I_p^{-0.84 \pm 0.11}$ with $R^2 = 0.762$.

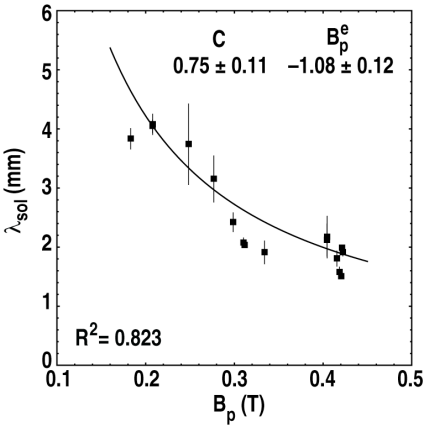

Fig. 1. Plot of λ_{sol} versus B_p together with a power law scaling, $\lambda_{sol} = C \cdot B_p^e$.

The strong dependence of the SOL heat flux width with B_p vastly restricts the possible models for transport in this region. There are two models in particular that strongly depend on B_p. The first is a heuristic model proposed by Goldston [3] in which magnetic field drifts carry particles across the separatrix into the SOL where parallel flows transport them to the divertor. The characteristic penetration depth into the SOL is of the order of the

poloidal gyroradius. The DIII-D data is in very good agreement with this model as shown in Fig. 2 which plots the measured λ_{sol} against $\lambda_{Goldston}$.

An alternative model proposes that the edge pressure rises until an MHD mode, such as the kinetic ballooning mode, is destabilized, limiting further increases in the pressure as well as its gradient. This establishes a critical pressure gradient that extends up to the separatrix and, it is hypothesized, all the way into the SOL. Fig. 3 shows evidence for this model. It is a plot of the measured pressure gradient at the separatrix versus the plasma current, I_p. A proxy for the critical pressure gradient is obtained from the infinite-n ballooning limit, which is a good approximation when there is no second-stable access [6]. The critical gradient obtained in this way is also shown in Fig. 3.

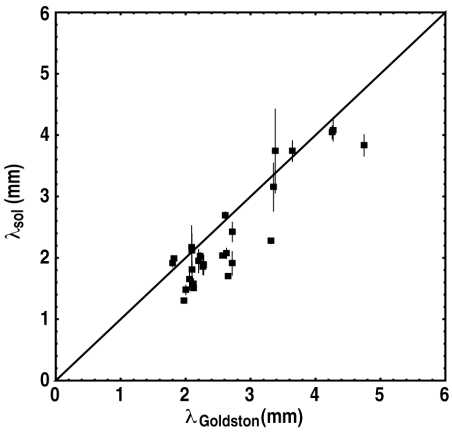

Fig. 2. Plot of λ_{sol} versus $\lambda_{Goldston}$ (from reference [3]) showing very good agreement between the two quantities.

The measured electron and critical pressure gradients trend in the same way, but differ by 50% in magnitude, which is well within the error bars of the measurement and simple ballooning model used. Better agreement is obtained if the ion pressure gradient is included assuming $dT_i / dR = dT_e / dR$.

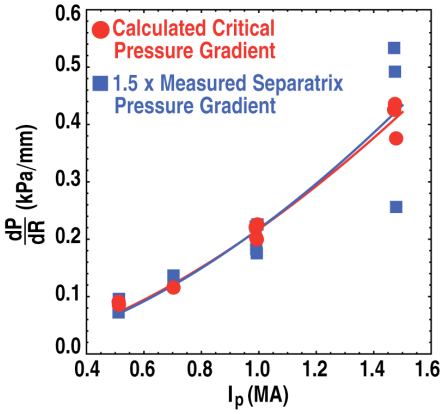

Fig. 3. Comparison of the measured electron pressure gradient at the separatrix and the infinite-n ballooning mode critical pressure gradient as a function of plasma current. The two quantities have a very similar dependence on I_p.

3. Profile measurements and power flow

Profiles of electron density and temperature as a function of plasma current, I_P, and normalized plasma density (Greenwald fraction, f_G) have been obtained using the recently upgraded Thomson scattering. An example of the pedestal/SOL portion of the electron density and temperature profiles, together with fits to the data (solid lines) is shown in Fig. 4 for low- and high-central-density cases. Also shown are lines tangent to the point of maximum gradient in the pedestal (dotted lines). The slope of both the density and temperature profiles in the pedestal region is extremely linear. Lines asymptotic to the point of maximum slope are also shown.

Power balance, based on two-point models of flux-limited and conduction-limited parallel transport [4], is used to infer the location of the separatrix. In the flux-limited model

$$q_{\text{flux-limited}} = \alpha e \left(\frac{e}{m}\right)^{1/2} nT^{3/2} \quad , \tag{1}$$

where α is a dimensionless constant with value ~ 0.3, e is the electron charge, m is the mass, n is the density, and T is the temperature.

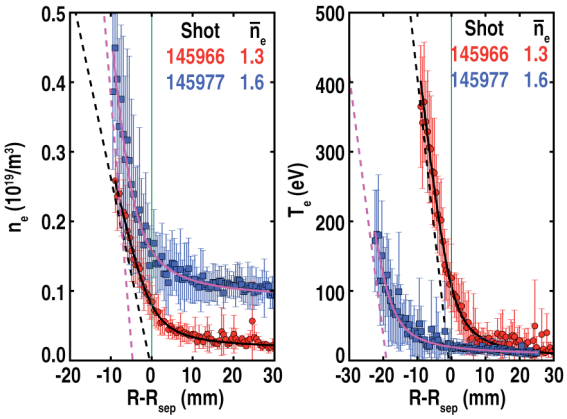

Fig. 4. Comparison of profiles of electron temperature and density at low and high central density obtained with the upgraded DIII-D Thomson scattering system. Fits to the SOL portion of the profile (solid lines) and lines parallel to the point of maximum slope (dashed lines) are also shown. The pedestal density gradient increases, as indicated by the lines asymptotic to the point of maximum slope, with increasing central density while the temperature gradient remains nearly constant.

For DIII-D, ions in the pedestal/SOL are found to always be in the flux-limited regime by virtue of their high temperature and consequent low collisionality (which is also lower than that of the electrons by $\sqrt{m_e / m_i}$). Alternatively, for the conduction-limited (Spitzer) model

$$q_{\text{cond-limited,e}} = \kappa_{0e} T_e^{5/2} \frac{dT_e}{d\ell_{\parallel}}$$

$$\cong \frac{2}{7} \kappa_{0e} T_e^{7/2} / L_{\parallel} \quad , \tag{2}$$

where κ_{0e} is a constant ($\kappa_{0e} \approx 2000 / Z_{eff}$) and $\ell_{\parallel}$ is the parallel path length along a field line which is approximated by the connection length, $L_{\parallel}$. Electrons may be in either the conduction- or flux-limited regimes dependent on their collisionality. The two-point models also provide a simple method for relating the heat flux width to profile scale lengths [7]. Their relation to the heat flux width can be found from Eqns. (1) and (2) and leads to the following relations

$$\lambda_{q,cond} = \frac{2}{7} L_{T_e} \quad , \tag{3}$$

$$\lambda_{q,\text{flux}} = \left(\frac{1}{L_{n_e}} + \frac{3/2}{L_{T_e}} \right)^{-1} \quad , \tag{4}$$

where L_{n_e} and L_{T_e} are gradient scale lengths of the density and temperature profiles evaluated at the separatrix.

In order to determine the separatrix location, Eqs. (1) and (2) are evaluated for the electrons as a function of radius using the measured profiles assuming that ½ the power through the SOL goes into the electron channel. Ions are neglected in the following for several reasons. First, the ion temperature profile is not known in the SOL. Attempts to linearly extrapolate the profile to zero based on its gradient at the separatrix or by fitting a tanh function to the pedestal portion of the profile yield very high temperatures far into the SOL. This in turn results a significant fraction of the power flowing through the ion channel and unrealistically low values for the separatrix electron temperature (< 10 eV). Alternatively, an exponential decay can be assumed, but the scale length is unknown and thus must be chosen arbitrarily.

Two cases result: flux-limited and conduction-limited parallel transport for the electrons. Using the measured electron profiles, the total power through the SOL is computed as a function of major radius

$$P_j(R) = A_\perp q_{j,e}(R),$$

$$j = cond,\ flux \quad , \tag{5}$$

where $A_\perp$ is the plasma surface area. The point on each of the curves that equals the measured power through the scrape-off-layer, P_{sol}, is used to establish the separatrix location for that model. Figure 5 plots the ratio of $\lambda_{q,cond}$ and $\lambda_{q,flux}$ evaluated at the separatrix to $\lambda_{sol,fit}$ where $\lambda_{sol,fit}$ is obtained from the scaling law of Fig. 1 (based on measurements). The flux-limited width is in better agreement with the measurements as the ratio is closer to unity (green horizontal line).

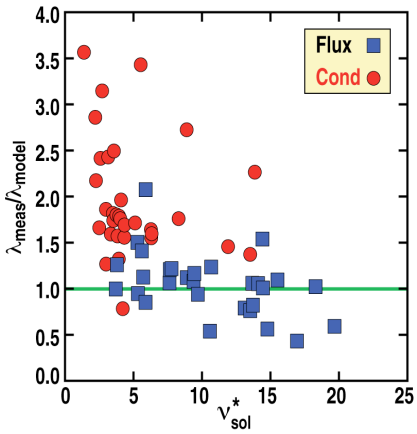

Fig. 5. Plot of the ratios $\lambda_{fit,sol} / \lambda_{cond}$ (red circles) and $\lambda_{fit,sol} / \lambda_{flux}$ (blue squares) versus B_p where $\lambda_{fit.sol}$ is from the scaling law of Fig. 1. The flux-limited ratio is closer to unity (green line) than the conduction-limited ratio.

Data has been obtained as a function of plasma current, I_p, and central density as measured by the Greenwald fraction, f_G, so that the dependence of $n_{e,sep,j}$ and $T_{e,sep,j}$ on these quantities can be derived. This is shown in Fig. 6, which plots $n_{e,sep,j}$ and $T_{e,sep,j}$ for conduction- (red circles) and flux-limited (blue squares) parallel heat transport versus I_p and f_G together with linear fits to selected data. The trends, when they exist, for the two cases are generally similar. The sepatrix density increases with increasing plasma current, I_p, for both models, which is to be expected as the confinement scales as I_p. There is no clear trend for either model when the separatrix density is plotted versus f_G. In contrast, the separatrix electron temperature is essentially independent of I_p but appears to decreases with f_G. The predicted flux-limited electron temperature is about twice as large as the conduction-limited electron temperature.

The difference in the location of separatrix is not that great for the two models, being around 2-3 mm as shown in Fig. 7 which plots the difference as a function of the f_G. However, this can make a difference of a factor of 2 in T_e (see Fig. 6). The conduction-limited separatrix location is always at greater major radius than the flux-limited separatrix location. This results from the strong dependence of the conduction-limited power flow on T_e, biasing the location to lower values of T_e and thus greater major radius.

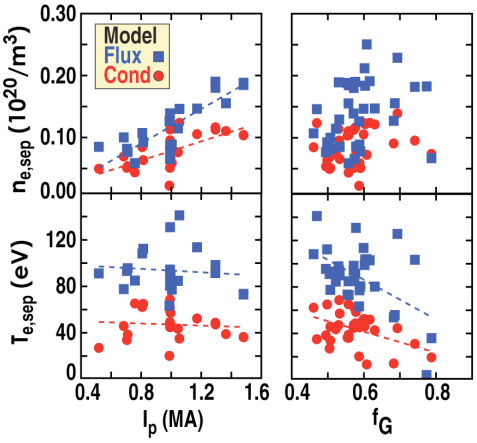

Fig. 6. Plots of $n_{e,sep,j}$ and $T_{e,sep,j}$ versus I_p and f_G for both conduction- (red circles) and flux-limited (blue squares) parallel heat transport models. Linear fits to selected data (dashed lines) are also shown. Although clear dependencies on I_p and f_G are not always observed, the predictions of the models are clearly differentiated.

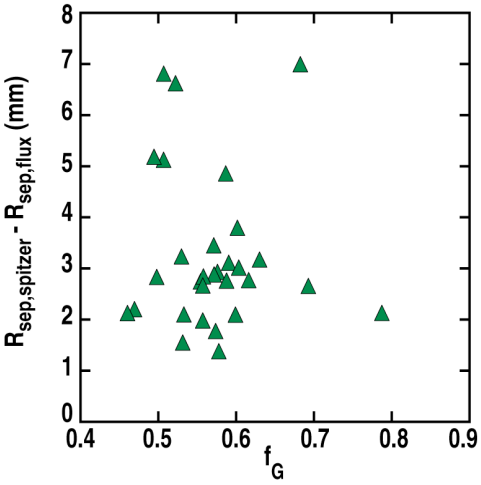

Fig. 7. Plot of the difference between the conduction- and flux-limited inferred location of the separatrix as a function of f_G. The conduction-limited location is always as large major radius than that of the flux-limited model due to its strong dependence on T_e.

4. Summary

The measured heat flux width is found to depend strongly on B_p and is essentially independent of all other engineering and physics parameters. The dependence for DIII-D is $\sim B_p^{-1}$ whereas for the joint data it is stronger going $\sim B_p^{-1.5}$. There are few theoretical models that predict such a dependence. One is a heuristic drift-based model that is in very good agreement with the measured heat flux width. Another is a critical gradient model in which the critical gradient extends into the SOL. While the model is still incomplete, there is some experimental evidence supporting it, as the measured electron pressure gradient and infinite-n ballooning mode critical gradient have a similar dependence on the plasma current.

The upgraded DIII-D Thomson scattering system makes detailed measurements of the pedestal and SOL profiles possible. This in turn has allowed us to make improved comparisons with a variety of theoretical models of the edge plasma. The simplest models considered are two-point models (flux-limited and conduction-limited) that relate power through the SOL to parallel heat transport in the SOL. These models yield predictions of the location of the separatrix and of the heat flux width. The flux-limited model is in better agreement with the measured heat flux width.

Acknowledgment

This work was supported by the US Department of Energy under DE-AC52-07NA27344, and DE-FC02-04ER54698.

References

[1] D.N. Hill, *et al.*, Rev. Sci. Instrum. **59**, (1988) 1878.
[2] M.A. Makowski, *et al.*, "Analysis of a multi-machine database for divertor heat fluxes", accepted for publication in Physics of Plasmas.
[3] R.J. Goldston, Nucl. Fusion **52** (2012) 013009.
[4] P.C. Stangeby, et. al., Nucl. Fusion **50**, 125003 (2010).
[5] T. Eich, *et al.*, Phys. Rev. Lett. **107**, (2011) 215001.
[6] P.B. Snyder and G.W. Hammet, Phys. Plasmas **8** (2001) 744.
[7] P.C. Stangeby, *The Plasma Boundary of Magnetic Fusion Devices*, Taylor and Francis Group 2000. ISBN 978-0-7503-0559-4.